IR Spectroscopy

DOI: 10.1002/ange.201205990

Tunneling and Tunneling Switching Dynamics in Phenol and Its Isotopomers from High-Resolution FTIR Spectroscopy with Synchrotron Radiation**

Sieghard Albert, Philippe Lerch, Robert Prentner, and Martin Quack**

Dedicated to Wilfred van Gunsteren on the occasion of his 65th birthday

The tunnel effect in chemical reactions[1] is one prominent example where it is obvious that the classical molecular dynamics description for chemistry and biochemistry[2] has to be amended by quantum dynamical effects. Some recent prototypical and well-studied examples include tunneling in $(HF)_2$ rearrangements,[3,4] mode selective control of stereomutation kinetics in HOOH,[5] and further prototypical reactions such as OH + CO[6] and kinetic control by tunneling in methylhydroxycarbene.[7] A particularly intriguing recent development is the theoretical prediction of tunneling switching in ClOOCl.[8,9] Here, at low energy, tunneling is completely suppressed by a very slight but dominant asymmetry arising from electroweak parity violation,[10] which effectively localizes the molecular wavefunction at the structure of one enantiomer at low energies. At higher energy, tunneling becomes dominant, thus switching the dynamics to a delocalized quantum wavefunction.[8,9] Because of the extremely tiny parity-violating asymmetry, the energy difference between enantiomers is predicted to be on the order of 10^{-11} J mol^{-1} or 100 aeV (equivalent to 25 mHz[11]), depending upon the molecule, and this effect has not yet been observed to date. For that reason we have conducted a study of tunneling in phenols, where, by means of isotopic substitution, a much larger asymmetry can be induced in the effective potential, but it is still small enough to observe tunneling switching at higher torsional excitation. We report here the first rotationally resolved Fourier transform infrared (FTIR) spectra of the excited torsional states of ordinary phenol (C_6H_5OH) in the THz domain. This has become possible by recent developments in FTIR spectroscopy using intense synchrotron radiation with a prototype spectrometer built for our group by Bruker.[12–14] In a second step these spectra are analyzed in terms of a recent theory making use of the quasiadiabatic channel reaction path Hamiltonian (RPH) approach[5,9] (see also references [15–17] for earlier developments). Finally, this calibrated theoretical approach is then used to predict tunneling switching for the *ortho*-deuterophenol isotopomer 2-C_6H_4DOH.

Ordinary phenol has a planar geometry with C_s point-group symmetry.[18,19] The tunneling barrier V/hc separating the two symmetrically equivalent structures is about 1200 cm^{-1}, and the tunneling between the two structures by internal rotation or torsion of the OH group leads to a splitting of 56 MHz in the vibrational ground state between the sublevels $\sigma = 0$ of A_1 symmetry and $\sigma = 1$ of B_2 symmetry as observed by microwave spectroscopy. This method also provided an initial value of the splitting of 0.09 cm^{-1} in the first torsional excited state as well as structural parameters[19–22] (see Figure 1, which anticipates some of the results). Low-resolution IR spectroscopy of phenol is also well known.[23,24] When tunneling is included, the ("nonrigid") molecular symmetry group M_{S4} of order 4 can be used, which is isomorphous to C_{2v}, to classify the vibration–rotation–tunneling (vrt) levels (Table 1).[24–26] Here E, C_2, σ_{xz}, and σ_{yz} are the point-group elements of C_{2v}, and J, K_a, K_c the rotational quantum numbers of an asymmetric top molecule for the ground state. E^* is the inversion of the axis system at the origin and $(\alpha\beta)$ the permutation of the symmetrically

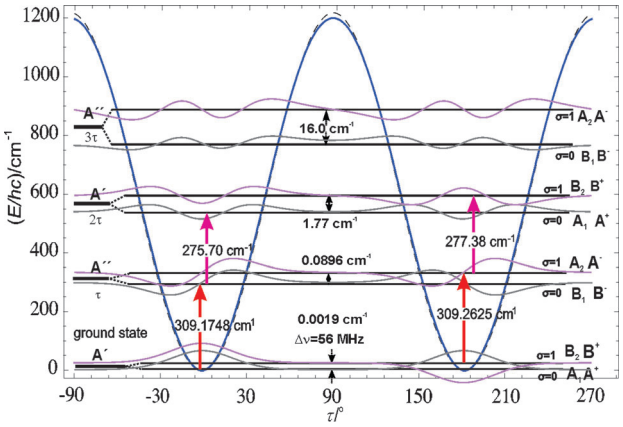

Figure 1. Vibrational term value diagram of the torsional band of phenol, including the electronic Born–Oppenheimer potential (dashed) and the lowest adiabatic channel potential (bold), both shifted to $E = 0$ at the minimum. The analyzed bands are indicated by arrows. The wavefunctions are delocalized.

[*] Dr. S. Albert, R. Prentner, Prof. M. Quack
Physical Chemistry, ETH Zurich
8093 Zürich (Switzerland)
E-mail: albert@ir.phys.chem.ethz.ch
martin@quack.ch
Dr. P. Lerch
Swiss Light Source, Paul-Scherrer-Institute
5332 Villigen (Switzerland)

[**] We thank Dr. Axel Keens for helpful discussions and Luca Quaroni for help. Our work is supported financially by the Schweizerischer Nationalfonds, ETH Zürich, and the European Research Council (ERC).

Supporting information for this article is available on the WWW under http://dx.doi.org/10.1002/anie.201205990.

Table 1: Character table for the C_{2v} and M_{S4} symmetry groups of phenol[25–29] with conventional definitions of the symbols. $\Gamma(S^*)$ gives the symmetry species in the subgroup $S^* = (E, E^*)$ isomorphous to C_s with correlations (A', A^+) and (A'', A^-).

C_{2v}		E	C_2	σ_{xz}	σ_{yz}			J	K_aK_c
	S_2^* M_{S4}	E	$(\alpha\beta)$	$(\alpha\beta)^*$	E^*	$\Gamma(S^*)$			
A_1	A^+	1	1	1	1	A^+	z		*ee*
A_2	A^-	1	1	−1	−1	A^-		J_z	*eo*
B_1	B^-	1	−1	1	−1	A^-	x	J_y	*oo*
B_2	B^+	1	−1	−1	1	A^+	y	J_x	*oe*

equivalent nuclei of the phenyl frame. The notation for symmetry species of M_{S4} makes the parity explicit in the exponent $(+,-)$.[26,27] The coordinate system for phenol was chosen so that the z-axis lies in the plane of the molecule along the CO bond, the y-axis perpendicular to the z-axis in the plane of the molecule, and the x-axis perpendicular to the plane of the molecule.[28,29]

The FTIR spectra of phenol were recorded with the ETH-SLS Bruker prototype 2009[12–14] using synchrotron radiation in the range 200 to 340 cm^{-1} in a 3 m glass cell at 296 K. This prototype spectrometer has an unapodized resolution corresponding to an instrumental bandwidth of 0.00053 cm^{-1} (16 MHz), which is currently the highest for a FTIR spectrometer worldwide.[12–14] Figure 2 shows the torsional fundamental spectrum including the torsional hot bands. The corresponding term value diagram is illustrated in Figure 1. Apertures from 1.8 mm down to 0.8 mm, which allow an effective instrumental resolution of 0.0007 cm^{-1}, were applied. The sample pressure was varied from 0.02 to 0.2 mbar excluding substantial pressure broadening. The Doppler width of phenol is 0.0004 cm^{-1} at 300 cm^{-1} and 296 K.

The first hot band centers can be assigned as $(v = 2^{\sigma=0} \leftarrow v = 1^{\sigma=0})$ at 275.70 cm^{-1} and $(v = 2^{\sigma=1} \leftarrow v = 1^{\sigma=1})$ at 277.38 cm^{-1}. These values are obtained from the Q-branch heads but have been confirmed by a partial high resolution line assignment. They agree with the low-resolution values from Bist et al.[23] However, a detailed look at the Q branches of the second torsional hot band shows three Q branches. The Q branches at 254.12 cm^{-1} and at 244.32 cm^{-1} illustrate a similar band shape as opposed to the shape of the Q branch at 237 cm^{-1}. For that reason the assignment $3^1 \leftarrow 2^1$ at 254.12 cm^{-1} and $3^0 \leftarrow 2^0$ at 237 cm^{-1} as described in reference [23] is questionable. For a more detailed analysis the P and R branches have to be analyzed. The assignment of the observed rovibrational transitions belonging to the two torsional subbands consisting of P and R branches has been carried out with a Loomis–Wood assignment program successfully used so far for the analysis of the FTIR spectra of the aromatic molecules pyridine[12,14] and pyrimidine.[30] The nuclear spin statistical weights for the subband $\sigma = 0$ show the intensity ratio *ee*:*eo*:*oo*:*oe* = 10:10:6:6 and for $\sigma = 1$ the intensity ratio *ee*:*eo*:*oo*:*oe* = 6:6:10:10 observed in each K_c series as an alternation of the transition intensity depending on the K_a value. Using this intensity alternation, it was possible to assign the K_c subseries as $\sigma = 0$ and $\sigma = 1$. Practically, for each J and K_a value two absorption lines are found with an intensity ratio 10:6, which is reversed at the next higher or lower J value. The advantage of *c*-type transitions consists of the observation of nuclear spin statistical weights even with a non-resolved asymmetry splitting.

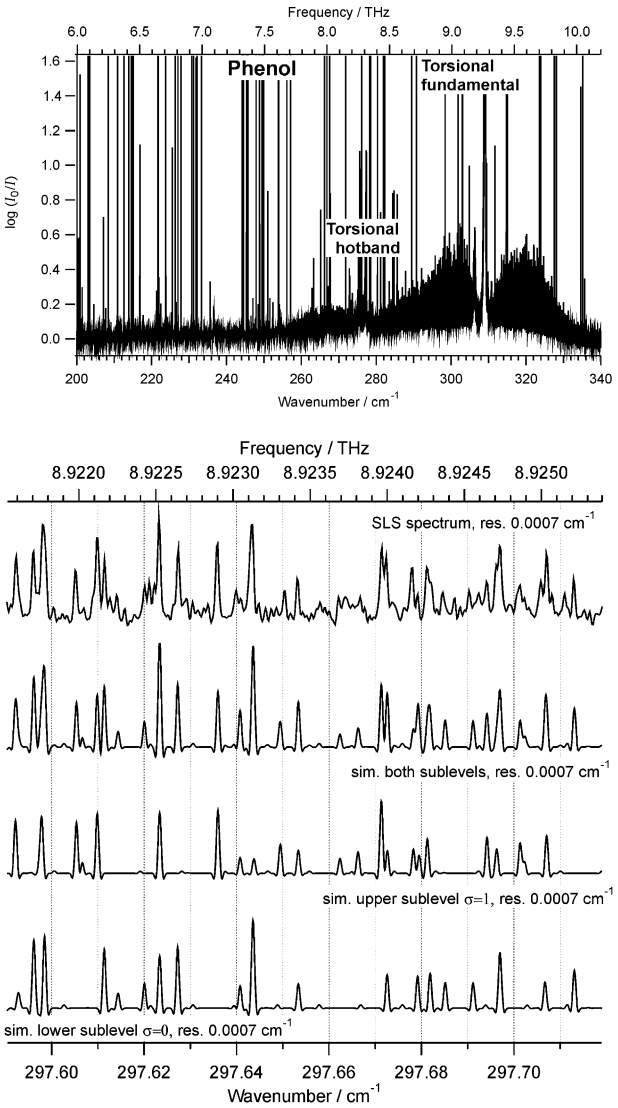

Figure 2. Upper part: The SLS-FTIR survey spectrum of the torsional fundamental of phenol (200–340 cm^{-1}) taken at a temperature of 296 K, a pressure of 0.2 mbar and path length of 3 m. Lower part: Comparison of part of the P-branch of the torsional fundamental of phenol with a simulation. R-branch sections are shown in the Supporting Information.

The rovibrational analysis was carried out with Watson's *A* reduced effective Hamiltonian[31–33] in the I^r representation up to quartic centrifugal distortion constants for each torsional subband. The spectroscopic data were analyzed using the WANG program.[32,33] The constants for the two torsional sublevels were used as ground-state constants. However, only the rotational constants A, B, C and the quartic constants Δ_J and Δ_{JK} of the two torsional levels in the ground state were fixed to their values during the fitting procedure. The quartic constants Δ_K, δ_J, and δ_K of the two torsional levels in the

ground state as well as the rotational constants A, B, C and the quartic constants Δ_J, Δ_K, δ_J, and δ_K of the two torsional sublevels in the first torsional excited state were newly determined. The values of the two quartic constants Δ_{JK} were held fixed to the values of the ground state. The constants of the ground state are listed in the Supporting Information, together with all assigned lines and those of the excited state in Table 2. 2200 lines were used for the fitting procedure. The

Table 2: Experimental rovibrational parameters of the two tunneling levels $\sigma=0$ (lower) and $\sigma=1$ (upper) of the first excited torsional state of phenol from the analysis of high-resolution spectra.

	Torsional state $v_\tau=1$[a] $\sigma=0$	Torsional state $v_\tau=1$[a] $\sigma=1$
$\tilde{\nu}_0$ [cm^{-1}]	309.174798 (11)	309.264360 (13)
A [cm^{-1}]	0.188447370 (26)	0.188416923 (23)
B [cm^{-1}]	0.08721326 (79)	0.08721315 (89)
C [cm^{-1}]	0.0596832 (11)	0.0596831 (56)
Δ_J [$\times10^{-9}$ cm^{-1}]	4.830 (97)	4.679 (97)
Δ_{JK} [$\times10^{-9}$ cm^{-1}]	3.9378	4.6562
Δ_K [$\times10^{-9}$ cm^{-1}]	31.56 (11)	29.481 (99)
δ_J [$\times10^{-9}$ cm^{-1}]	1.23 (56)	2.96 (56)
δ_k [$\times10^{-9}$ cm^{-1}]	20.1 (15)	13.6 (16)
N_{data}	2200	
d_{rms} [cm^{-1}]	0.00014	

[a] The uncertainties are given in terms of one sigma in parentheses. Parameters without uncertainties are fixed to the values of[21] See also for ground-state constants given in the Supporting Information.

rotational constants do not change dramatically upon excitation of the torsional mode and the quartic constants change only slightly. This is another indication that the rotational–torsional interaction can be neglected in a first approximation, as the root-mean-square deviation of $d_{rms}=0.00014$ cm^{-1} indicates. The torsional fundamental of phenol was simulated using the constants derived here and including the nuclear spin statistical weights. Figure 2 (lower part) shows a comparison of a measured part of the P-branch regions of the torsional fundamental (lower part, upper trace) with a simulation (lower part, second trace). The simulation consists of the two simulated torsional subbands shown in the third and lower trace in the lower part of Figure 2. As can be seen, the agreement between measured and simulated spectrum is good considering the neglect of other hot bands and ^{13}C isotopomers.

Frequencies and torsional splittings were calculated using our modified version of the quasiharmonic reaction path Hamiltonian approach.[5,34,35] This method was already successfully used for the description of the torsion in H_2O_2[5,34] and the inversion in aniline.[35] In this RPH approximation, the torsion is treated exactly and is coupled to a bath of harmonic oscillators. The torsional potential was calculated at the CCSD(T) level of theory using the cc-pVTZ basis set at geometries optimized at the B3LYP/6-311++G** level of theory. Starting from the optimized geometry, the dihedral C-C-O-H angle was frozen every 5 degrees, while bond lengths, angles, and harmonic normal mode frequencies were recalculated (clamped coordinate approach) using tight convergence criteria; no empirical fitting is employed during any stage of

Table 3: Comparison of the torsional transition wavenumbers, splittings, and transition times τ within the torsional polyad of phenol derived from the experimental data with the calculated values using the RPH approximation.

Assignment	$\tilde{\nu}$(exp.) [cm^{-1}]	$\tilde{\nu}$(calc.) [cm^{-1}]	τ_{calc}/ps = $h/(2\Delta E)$
$0^1\leftarrow0^0$	0.0019	0.0013	12829.39
$1^0\leftarrow0^0$	309.17	309.07	
$1^1\leftarrow1^0$	0.0896	0.070	238.26
$2^0\leftarrow1^0$	275.70	273.58	
$2^1\leftarrow2^0$	1.77	1.49	11.19
$3^0\leftarrow2^0$	[a]	230.91	
$3^1\leftarrow3^0$	[a]	15.85	1.05

[a] Not yet clearly identified by experiment at high resolution.

the calculation. Table 3 shows a comparison of the experimental and calculated torsional transition wavenumbers and splittings. As can be seen, the agreement between experimental and calculated splittings is excellent given that the potential was not empirically adjusted.

Finally, we show in Figure 3 the asymmetric lowest adiabatic channel potential and the torsional levels for *ortho*-deuterophenol. The asymmetry arises mainly from the change of zero point energy along the reaction path leading to a shift of 7.19 cm^{-1} in the quasiadiabatic channel minimum. Although the calculations predict transition frequencies very similar to those of the undeuterated species, the asymmetry leads to qualitatively different molecular wavefunctions. For lower energies (v=0,1) localized eigenstates are found, whereas for higher torsional excitation ($v=3$) the wavefunctions are delocalized eigenstates as in the undeuterated

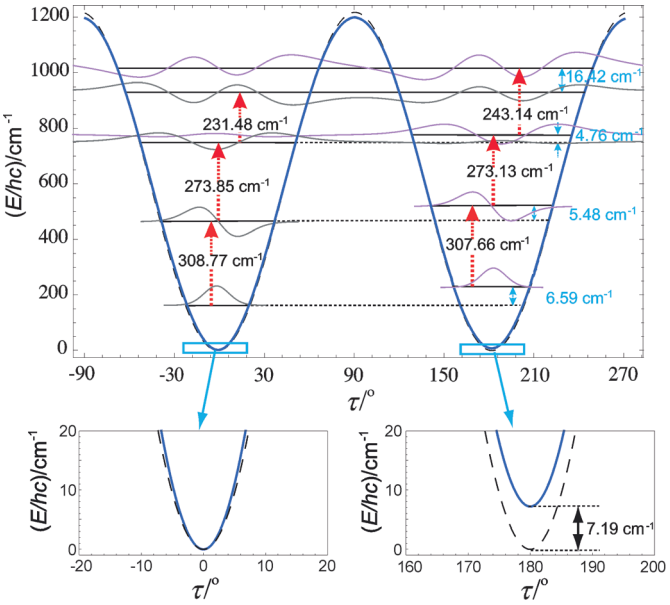

Figure 3. The electronic Born–Oppenheimer potential (dashed) and the lowest adiabatic channel potential (bold) for 2-C_6H_4DOH including the excited torsional levels. The enlargement at the minimum illustrates the asymmetry of the double well potential arising from the change in zero point energy. The lowest wavefunctions are each localized in one of the wells.

species. In the case of lower excitation, the absorption lines of two slightly different rotamers that have already been reported for the microwave region are found in the spectrum.[36,37] In the case of higher excitations absorption lines for the delocalized state should also be detected. Although the predictions for *ortho*-deuterophenol might not be quantitatively accurate, they should be sufficient to derive the order of magnitude, thus predicting definitely the possibility of tunneling switching. According to our calculations, this phenomenon can also be predicted for *meta*-deuterophenol and even for phenol substituted with ^{13}C in the *ortho* position, although the zero-point energy effect is predicted to be smaller in these two cases.

We have also studied the dependence of the torsional tunneling upon excitation of other vibrational modes. The situation seems to be more complex than in the case of H_2O_2 and aniline studied previously, and we shall report on these results separately.

In summary, the use of bright synchrotron light in the THz region in combination with a very highly resolving FTIR interferometer made it possible to rotationally resolve the IR spectrum of phenol. It was possible to identify the torsional splitting of the torsional states confirmed by calculation using the quasiadiabatic channel RPH method. The present work demonstrates how to study a whole class of "chemical reactions by tunneling switching" through high-resolution IR spectroscopy.

Received: July 26, 2012
Published online: December 6, 2012

Keywords: high-resolution IR spectroscopy · phenol · synchrotron radiation · THz spectroscopy · tunneling kinetics

[1] F. Hund, *Z. Phys.* **1927**, *43*, 805 – 826.
[2] W. F. van Gunsteren, D. Bakowies, R. Baron, I. Chandrasekhar, M. Christen, X. Daura, P. Gee, D. P. Geerke, A. Glattli, P. H. Hunenberger, M. A. Kastenholz, C. Ostenbrink, M. Schenk, D. Trzesniak, N. F. A. van der Vegt, H. B. Yu, *Angew. Chem.* **2006**, *118*, 4168 – 4198; *Angew. Chem. Int. Ed.* **2006**, *45*, 4064 – 4092.
[3] W. Klopper, M. Quack, M. A. Suhm, *J. Chem. Phys.* **1998**, *108*, 10096 – 10115.
[4] C. Manca, M. Quack, M. Willeke, *Chimia* **2008**, *62*, 235 – 239.
[5] B. Fehrensen, D. Luckhaus, M. Quack, *Chem. Phys.* **2007**, *338*, 90 – 105.
[6] T. L. Nguyen, B. C. Xue, R. E. Weston, J. R. Barker, J. F. Stanton, *J. Phys. Chem. Lett.* **2012**, *3*, 1549 – 1553.
[7] P. R. Schreiner, H. R. Reisenauer, D. Ley, D. Gerbig, C.-H. Wu, W. D. Allen, *Science* **2011**, *332*, 1300 – 1303.
[8] M. Quack, M. Willeke, *J. Phys. Chem. A* **2006**, *110*, 3338 – 3348.
[9] R. Prentner, M. Quack, J. Stohner, M. Willeke, *Faraday Discuss.* **2011**, *150*, 130 – 132.
[10] R. Berger, M. Gottselig, M. Quack, M. Willeke, *Angew. Chem.* **2001**, *113*, 4342 – 4345; *Angew. Chem. Int. Ed.* **2001**, *40*, 4195 – 4198.
[11] M. Quack, *Faraday Discuss.* **2011**, *150*, 533 – 565.
[12] S. Albert, M. Quack, *ChemPhysChem* **2007**, *8*, 1271 – 1281.
[13] S. Albert, K. Keppler Albert, P. Lerch, M. Quack, *Faraday Discuss.* **2011**, *150*, 71 – 99.
[14] S. Albert, K. Keppler Albert, M. Quack in *Handbook of High Resolution Spectroscopy*, *Vol. 2* (Eds.: M. Quack, F. Merkt), Wiley, Chichester, **2011**, pp. 965 – 1019.
[15] L. Hofacker, *Z. Naturforsch. A* **1963**, *18*, 607 – 619.
[16] M. Quack, J. Troe, *Ber. Bunsen-Ges.* **1974**, *78*, 240 – 252; M. Quack, J. Troe in *Encyclopedia of Computational Chemistry*, *Vol. 3* (Eds.: P. v. R. Schleyer, N. Allinger, T. Clark, J. Gasteiger, P. A. Kollman, H. F. Schaefer, P. R. Schreiner), Wiley, New York, **1998**, pp. 2708 – 2726.
[17] W. H. Miller, N. C. Handy, J. E. Adams, *J. Chem. Phys.* **1980**, *72*, 99 – 112.
[18] S. Albert, K. Keppler Albert, P. Lerch, M. Quack, *Faraday Discuss.* **2011**, *150*, 517 – 519.
[19] E. Mathier, D. Welti, A. Bauder, H. H. Günthard, *J. Mol. Spectrosc.* **1971**, *37*, 63 – 76.
[20] T. Kojima, *J. Phys. Soc. Jpn.* **1960**, *15*, 284 – 287; H. Forest, B. P. Dailey, *J. Chem. Phys.* **1966**, *45*, 1736 – 1746.
[21] C. Tanjaroon, S. G. Kukolich, *J. Phys. Chem. A* **2009**, *113*, 9185 – 9192.
[22] N. W. Larsen, F. M. Nicolaisen, *J. Mol. Struct.* **1974**, *22*, 29 – 43.
[23] H. D. Bist, J. Brand, D. R. Willams, *J. Mol. Spectrosc.* **1967**, *24*, 402 – 412.
[24] H. W. Wilson, R. W. Macnamee, J. R. Durig, *J. Raman Spectrosc.* **1981**, *11*, 252 – 255.
[25] H. C. Longuet-Higgins, *Mol. Phys.* **1963**, *6*, 445 – 460.
[26] M. Quack in *Handbook of High Resolution Spectroscopy*, *Vol. 1* (Eds.: M. Quack, F. Merkt), Wiley, Chichester, **2011**, pp. 659 – 722.
[27] M. Quack, *Mol. Phys.* **1977**, *34*, 477 – 504.
[28] G. Berden, W. L. Meerts, M. Schmitt, K. Kleinermanns, *J. Chem. Phys.* **1996**, *104*, 972 – 982.
[29] H. D. Bist, J. C. D. Brand, D. R. Williams, *J. Mol. Spectrosc.* **1966**, *21*, 76 – 98.
[30] S. Albert, M. Quack, *J. Mol. Spectrosc.* **2007**, *243*, 280 – 291.
[31] J. K. G. Watson in *Vibrational Spectra and Structure*, *Vol. 6* (Ed.: J. Durig), Elsevier, Amsterdam, **1978**, pp. 1 – 89.
[32] D. Luckhaus, M. Quack, *Mol. Phys.* **1989**, *68*, 745 – 758.
[33] S. Albert, K. Keppler Albert, H. Hollenstein, C. Manca Tanner, M. Quack in *Handbook of High-Resolution Spectroscopy*, *Vol. 1* (Eds.: M. Quack, F. Merkt), Wiley, Chichester, **2011**, pp. 117 – 173.
[34] B. Fehrensen, D. Luckhaus, M. Quack, *Chem. Phys. Lett.* **1999**, *300*, 312 – 320.
[35] B. Fehrensen, D. Luckhaus, M. Quack, *Z. Phys. Chem. (Muenchen Ger.)* **1999**, *209*, 1 – 19.
[36] T. Pedersen, N. W. Larsen, L. Nygaard, *J. Mol. Struct.* **1969**, *4*, 59 – 77.
[37] N. W. Larsen, *J. Mol. Struct.* **1979**, *51*, 175 – 190.

